Minimal determinants for binding activated G-alpha from the structure of a G-alpha-i1/peptide dimer†

Christopher A. Johnston‡, Ekaterina S. Lobanova§, Alexander S. Shavkunov§, Justin Low‖, J. Kevin Ramer⊥, Rainer Blaesius⊥, Zoey Fredericks⊥, Francis S. Willard‡, Brian Kuhlman‖, Vadim Y. Arshavsky§, and David P. Siderovski*,‡

‡*Department of Pharmacology, University of North Carolina School of Medicine, Chapel Hill, North Carolina 27599-7365*

§*Department of Ophthalmology and Neurobiology, Duke University, Durham, North Carolina 27710*

‖*Department of Biochemistry & Biophysics, University of North Carolina School of Medicine, Chapel Hill, North Carolina 27599-7365*

⊥*Department of Karo Bio USA, Durham, North Carolina 27703*

Abstract

G-proteins cycle between an inactive GDP-bound state and active GTP-bound state, serving as molecular switches that coordinate cellular signaling. We recently used phage-display to identify a series of peptides that bind Gα subunits in a nucleotide-dependent manner [Johnston, C. A., Willard, F. S., Jezyk, M. R., Fredericks, Z., Bodor, E. T., Jones, M. B., Blaesius, R., Watts, V. J., Harden, T. K., Sondek, J., Ramer, J. K., and Siderovski, D. P. (2005) *Structure 13*, 1069–1080]. Here we describe the structural features and functions of KB-1753, a peptide that binds selectively to GDP·AlF₄⁻- and GTPγS-bound states of Gα$_i$ subunits. KB-1753 blocks interaction of Gα$_{transducin}$ with its effector, cGMP phosphodiesterase, and inhibits transducin-mediated activation of cGMP degradation. Additionally, KB-1753 interferes with RGS protein binding and resultant GAP activity. A fluorescent KB-1753 variant was found to act as a sensor for activated Gα in vitro. The crystal structure of KB-1753 bound to Gα$_{i1}$·GDP·AlF₄⁻ reveals binding to a conserved hydrophobic groove between switch II and α3 helices, and, along with supporting biochemical data and previous structural analyses, supports the notion that this is the site of effector interactions for Gα$_i$ subunits.

Heterotrimeric G-proteins serve as critical relays that transmit cues from extracellular stimuli as diverse as neurotransmitters, hormones, photons, and odorants/tastants to intracellular signaling cascades responsible for eliciting specific cellular effects (1,2). In the traditional model of G-protein signaling, cell surface G-protein coupled receptors (GPCRs), upon activation by the aforementioned stimuli, catalyze the exchange of GDP for GTP on the Gα

[1]Abbreviations: AlF₄⁻, aluminum tetrafluoride; CFP, cyan fluorescent protein; cGMP, cyclic guanosine monophosphate; FRET, fluorescence resonance energy transfer; GAP, GTPase-accelerating protein; GDP, guanosine diphosphate; GEF, guanine nucleotide exchange factor; GMP, guanosine monophosphate; GPCR, G protein-coupled receptor; GTP, guanosine triphosphate; PDE, phosphodiesterase; RGS, regulator of G-protein signaling; ROS, rod outer segment; SPR, surface plasmon resonance; YFP, yellow fluorescent protein.

subunit. This results in adoption of the active, GTP-bound Gα conformation, which dissociates from the Gβγ dimer formerly bound to inactive, Gα·GDP as a heterotrimeric Gαβγ complex. Gα·GTP and freed Gβγ then regulate a variety of downstream effectors by both individual and coordinated mechanisms (1,2). The GTP-dependent conformational changes within Gα required for effector binding are known for $G\alpha_s$ bound to adenylyl cyclase (3), $G\alpha_{transducin}$ ($G\alpha_t$) bound to the gamma subunit of cGMP phosphodiesterase (PDEγ) (4), $G\alpha_{13}$ bound to p115RhoGEF (5), and $G\alpha_q$ bound to GRK2 (6). However, no effector-bound structure of $G\alpha_{i1-3}$ has yet been determined. Gα·GTP signaling to effectors is terminated by intrinsic GTP hydrolysis activity of Gα, returning it to the GDP-bound conformation and Gβγ reassociation. GTP hydrolysis can be dramatically enhanced by the family of proteins known as 'regulators of G-protein signaling' (RGS), which serve as GTPase-accelerating proteins (GAPs) for Gα subunits (7,8). This model of nucleotide cycling predicts that the duration and intensity of signaling is ultimately determined by the lifetime of Gα in the activated, GTP-bound conformation. Therefore, a complete understanding of the molecular determinants of the guanine nucleotide cycle is of particular importance to understanding the temporal aspects governing G-protein-mediated signal transduction.

We recently employed phage display technology to identify peptides capable of interacting with Gα in a conformation-dependent manner (9,10). These peptides selectively bind Gα by distinguishing key structural orientations of the critical 'switch regions' in Gα that govern nucleotide exchange and hydrolysis and control interaction with regulatory proteins and effectors (11). In addition to their discriminatory binding properties, these peptides can possess intrinsic regulatory properties that provide insight into the regulation of Gα signaling. For example, we recently described the molecular basis for the interaction of a GDP-selective peptide, KB-752, with Gα·GDP (10). KB-752 serves as a guanine nucleotide exchange factor (GEF) *in vitro*, and the structure of the Gα/KB-752 complex provided insight into the role of switch II displacement in the mechanism of GPCR-mediated nucleotide exchange, a process that remains largely elusive (12–14). Several other groups have also used similar techniques to identify Gα- and Gβγ-binding peptides that have provided insight regarding the mechanics of heterotrimeric G-protein signaling (15–18).

Here we describe the crystal structure of a peptide, KB-1753, that interacts exclusively with activated $G\alpha_i$ subunits, including the closely related $G\alpha_{transducin}$. The structure of the KB-1753/$G\alpha_{i1}$·GDP·AlF_4^- complex reveals the molecular determinants of nucleotide selective binding of KB-1753 to Gα, highlighting the importance of the disposition of the switch II helix. KB-1753 competitively antagonizes the binding of PDEγ to $G\alpha_t$, suggesting that KB-1753 binds in a similar fashion to that of effectors. Additionally, KB-1753 prevents RGS protein binding and resultant GAP activity towards $G\alpha_{i1}$ and $G\alpha_t$. We also demonstrate the utility of a fluorescently-modified KB-1753 to serve as a sensor for activated $G\alpha_{i1}$ *in vitro*. Collectively, our results represent the first structure of $G\alpha_{i1}$ engaging an activation-state-selective target in its effector-binding region and underscore the usefulness of the KB-1753 peptide as a tool for studying G-protein signal transduction.

MATERIALS AND METHODS

Materials

Unless noted, all reagents were from Sigma. Peptides were synthesized by Anaspec (San Jose, CA), except for the C-terminal cysteine variant of KB-1753 and PDEγ (63–87) (GLGTDITVICPWEAFNHLELHELAQYGII), which were synthesized by the Tufts University Core Facility (directed by Dr. Michael Berne).

KB-1753/YFP plasmid construction

Oligonucleotides encoding KB-1753 were constructed with 5'-*Kpn*I and 3'-*Bam*HI overhangs: *sense:* 5'-CGT CTT CTC GAG GTT ACT ACC ATG GTA TTT GGG TGG GTG AAG AAG GTC GAC TTT CTC GAT GC-3' and *antisense:* 5'-GAT CGC ATC GAG AAA GTC GAC CTT CTT CAC CCA CCC AAA TAC CAT GGT AGT AAC CTC GAG AAG ACG TA C-3'. 100 ng of each primer were mixed, denatured, annealed (55°C for 1 min), and cooled prior to ligation into *Kpn*I/*Bam*HI-digested pEYFP-N1 (Clontech). To avoid steric hindrance to the KB-1753/Gα interaction by YFP, we inserted a flexible linker (Gly-Ser-Gly-Gly-Ser-Gly) between KB-1753 and YFP by insertional mutagenesis (QuickChange; Stratagene) with the following primers: *sense:* 5'-CGA CTT TCT CGA TGC GGA TCT GGT GGC TCA GGG GAT CCA CCG GTC GCC-3' and *antisense:* 5'-GGC GAC CGG TGG ATC CCC TGA GCC ACC AGA TCC GCA TCG AGA AAG TCG -3'. The KB-1753-linker-YFP open-reading frame was then isolated using PCR (30 cycles of: 95°C denaturing [30 sec], 55°C annealing [1 min], 72°C extension [1 min]) using the following primers: *sense:* 5'- TAC TTC CAA TCC AAT GCG TCT TCT CGA GGT TAC TAC CAT GGT ATT-3' and *antisense:* 5'- TTA TCC ACT TCC AAT GCG CTA CTT GTA CAG CTC GTC CAT GCC GAG AGT-3' and then subcloned into an N-terminal 6xHis-tagged vector using a ligation-independent strategy previously described (19).

Protein production

His$_6$-tagged N-terminal truncated human Gα$_{i1}$ (ΔN-Gα$_{i1}$), as well as full-length Gα$_{i2}$, Gα$_{i3}$, and Gα$_{oA}$ subunits, were purified from *E. coli* as previously described (20,21). His$_6$-tagged RGS12 RGS domain (aa 702 – 846 of SwissProt O08774) was cloned into pMCSG7 using a ligation-independent cloning strategy (19) and purified as described for Gα$_{i1}$. His$_6$-tagged human RGS16 (aa 53–190; ref. 22) was prepared from the expression construct pLIC-SGC1-RGS16-s001 obtained from SGC (Oxford), per their published protocol (PDB ID 2BT2). Transducin heterotrimer and PDE6 were purified from bovine retinas as described previously (23); urea-treated photoreceptor membranes used as the source of photoactivated rhodopsin were purified from bovine retinas as previously described (24).

Surface plasmon resonance

SPR binding assays were performed at 25°C using a BIAcore 3000. N-terminally biotinylated KB-1753 or PDEγ(63–87) peptides (diluted to 0.1 µg/ml in BIA-run buffer [10 mM HEPES (pH 7.4), 150 mM NaCl, 10 mM MgCl$_2$, 0.005% NP40]) were coupled to flow cells of streptavidin biosensors (Biacore) to a surface density of ~500 RU. Gα subunits were diluted in BIA-run buffer in the presence of 100 µM GDP, 100 µM GDP plus 30 µM AlCl$_3$ and 10 mM NaF, or 100 µM GTPγS and incubated at room temperature for 2 hours. Gα subunits in desired nucleotide states (30 µL) were then injected over flow cells at 10 µL/min, followed by a 300 s dissociation phase. To correct for nonspecific binding and buffer-shift artifacts, binding curves from a surface containing a control peptide (mNOTCH1; ref. 25) were subtracted from all binding curves. Surfaces were regenerated with two 10 µL injections of 500 mM NaCl plus 25 mM NaOH at 20 µL/min. BIAevaluation 3.0 was used for binding curve and kinetic analyses. Dissociation constants (K$_D$) were determined by saturation binding as previously described (20,21).

Crystallization and structure determination

ΔN-Gα$_{i1}$ protein (25 mg/ml in [20 mM Tris (pH 7.5), 1 mM MgCl$_2$, 20 mM NaCl, 1 mM DTT, 5% glycerol, 10 µM GDP, 30 µM AlCl$_3$, 10 mM NaF]) was incubated with a 1.5-fold molar excess of KB-1753 at room temperature for 5 min prior to screening. Initial crystals were obtained in condition 28 of the PEG-Ion Screen (Hampton Research) and refined to final crystallization conditions of 15% PEG-8000 and 0.3 M calcium acetate using the vapor

diffusion method with 8 µL hanging drops of a 1:1 volume ratio of protein to buffer. Crystals formed in 2–4 days at 4°C in the space group P3$_2$21 (*a* = *b* = 103.13 Å, *c* = 206.99 Å; α = β = 90°, γ = 120°) with two Gα$_{i1}$/KB-1753 heterodimers in the asymmetric unit. Crystals were cryoprotected in crystallization buffer supplemented with 20% glycerol for ~1 min, then submerged in liquid N$_2$. A 2.8 Å native data set was collected at Brookhaven National Laboratories using the x29 beamline. Data was scaled and indexed using HKL2000 (26). The structure of Gα$_{i1}$·GDP·AlF$_4^-$ (PDB ID 1GFI), excluding waters, GDP, and AlF$_4^-$, was used for molecular replacement (27). Initial solutions were found with correlation coefficients of 57.5 and starting R-factor of 47.6, which was reduced to 39.7 with an initial round of refinement. Model building was completed using O (28), with successive rounds of simulated annealing, minimization, B-group, and rigid body refinements being completed by CNS (29). Noncrystallographic symmetry restraints were used in initial cycles of refinement, and both Gα$_{i1}$/KB-1753 dimers were essentially identical. All electron density map calculations were completed with CNS. The N-terminal residues 25–32 of Gα$_{i1}$ were disordered along with residues 112–121 in the αB-αC loop of the all-helical domain; these segments were excluded in the final Gα$_{i1}$/KB-1753 model. All structural images were generated using PyMol (DeLano Scientific, San Carlos, CA).

PDE6 activity assays

PDE6 activity was measured as described (30). Briefly, illuminated ureatreated photoreceptor membranes (20 µl; 10 µM rhodopsin final), a source of photoexcited rhodopsin, were reconstituted with purified transducin (1 µM) at room temperature in buffer containing 10 µl GTPγS, 100 mM NaCl, 8 mM MgCl$_2$ and 10 mM Tris-HCl (pH 7.8). When needed, 20 µM of wildtype or mutant KB-1753 peptide was also added. PDE6 (0.05 µM) was added immediately before the reaction was initiated by 10 µl [^{3}H]cGMP (2.5 mM containing ~10^5 dpm/sample) and terminated by addition of 100 µl 0.1 M HCl. The mixture was then neutralized by 100 µl of 0.1 M Tris and incubated with 75 µl of king cobra snake venom (1 mg/ml) for 1 h to convert GMP to guanosine. The solution was then passed through an anion-exchange DEAE-Sepharose column to separate guanosine from cGMP, and washed twice with 0.8 ml of H$_2$O. The eluent was mixed with 10 ml ScintiSafe cocktail and radioactivity was measured by scintillation counting.

GTPase assays

Single-turnover GTPase assays with Gα$_{i1}$ were conducted as described (31). Briefly, 100 nM Gα$_{i1}$ was incubated at 30°C for 15 min in buffer C (50 mM Tris pH 7.5, 0.05% C$_{12}$E$_{10}$, 1 mM DTT, 5 µg/ml BSA, 10 mM EDTA, 100 mM NaCl) containing ~1×10^6 cpm of [γ-^{32}P]-GTP (6000 Ci/mmol). Samples were then placed on ice for 5 min. Reactions (on ice) were initiated by adding 10 mM MgCl$_2$ (with 100 µM GTPγS) and timed reaction aliquots were quenched by charcoal slurry (containing 20 mM H$_3$PO$_4$, pH 3) followed by centrifugation (~4000 ×g for 10 min at 4°C). Supernatants with free [γ-^{32}Pi] were analyzed by scintillation counting. Background counts (in the absence of Gα$_{i1}$) were subtracted from all experimental conditions.

Multiple-turnover GTPase assays with Gα$_t$ were conducted as described (32). Briefly, illuminated urea-treated photoreceptor membranes were mixed with transducin at room temperature in a buffer containing 100 mM NaCl, 8 mM MgCl$_2$, 10 mM Tris HCl pH 7.8 and 1 mM DTT. The reaction was started by the addition of 10 µl of [γ-^{32}P]GTP at desired concentration (final concentration 20 µM; approximately 10^5 dpm/sample) to 20 µl of membranes (final concentrations of 10 µM rhodopsin and 1 µM transducin) supplemented by additional proteins and/or peptides when needed. The reaction was stopped by 100 µl of 6% perchloric acid. ^{32}P$_i$ formation was measured with activated charcoal. In the experiment addressing the effect of PDEγ on RGS16 GAP activity, PDEγ (63–87) peptide was used instead of the full length PDEγ because this peptide completely substitutes for PDEγ in RGS protein

regulation but, unlike PDEγ, does not block repetitive transducin activation by rhodopsin (33).

Fluorescence resonance energy transfer (FRET) assays

FRET assays for Gα/RGS interaction, along with purification of $G\alpha_{i1}$-CFP and YFP-RGS4, were completed as described (34). $G\alpha_{i1}$-CFP was diluted in 10 mM Tris pH 8.0, 1 mM EDTA, 10 mM $MgCl_2$, 150 mM NaCl, and 10 µM GDP. Experiments on the effects of AlF_4^- activation were performed in buffer supplemented with 30 µM $AlCl_3$ and 10 mM NaF. Measurements were made with a LS-55B spectrofluorimeter (Perkin-Elmer). Emission scans were performed at 20 nm/min using excitation of 433 nm, with slit widths of 5 nm. Emission maxima used for CFP and YFP were 474 nm and 525 nm, respectively. For peptide competition experiments, $G\alpha_{i1}$ (200 nM) was allowed to incubate in the quartz cuvette with wildtype or mutant KB-1753 (2 µM) for 2 min prior to adding YFP-RGS4.

RESULTS

Identification of an activated-state-selective Gα binding peptide

To identify peptides capable of interacting with Gα selectively in the activated conformation, we performed phage display analysis as previously described for peptides that bind inactivated, GDP-bound Gα (9,10). Of the GTPγS-dependent $G\alpha_{i1}$ binding peptides obtained, seven peptides shared a consensus sequence of three hydrophobic residues centered around tryptophan and flanked by glycines (Figure 1A). A MOTIF search (http://motif.genome.jp/) of the Swiss-Prot protein database (35) with the degenerate sequence motif G-[IV]-W-[ILMSVW]-G revealed 166 proteins bearing this peptide signature across all represented genomes, but none was a known G-protein effector (data not shown). From this family of seven peptides, the longest and most avid binder, KB-1753, became the focus of our current efforts. To quantitate the nucleotide-dependent interaction of KB-1753 with $G\alpha_{i1}$, we performed surface plasmon resonance (SPR) measurements on a streptavidin biosensor coated with biotinylated KB-1753. Injection of $G\alpha_{i1}$·GDP·AlF_4^- or $G\alpha_{i1}$·GTPγS analytes yielded robust binding to KB-1753, whereas $G\alpha_{i1}$·GDP showed no detectable interaction (Figure 1B). To assess the affinity of these interactions, dissociation constants (K_D values) were obtained by saturation binding using a previously described technique (20,21). As shown in Figure 1C, $G\alpha_{i1}$ in both the transition state (GDP·AlF_4^-) and activated state (GTPγS) interacts with KB-1753 with low micromolar affinity. KB-1753 bound with highest affinity to $G\alpha_{i2}$·GDP·AlF_4^-, nearly 10-fold better than either $G\alpha_{i1}$ or $G\alpha_{i3}$ (Figure 1C). No appreciable affinity was detected for the GDP-bound conformation of any of these $G\alpha_i$ subunits, confirming the results of the original phage selection (10). A chimeric Gα subunit that closely mimics transducin ("αT*" in which the corresponding region from $G\alpha_{i1}$ was inserted between residues 215 and 294 of $G\alpha_t$; herein denoted $G\alpha_{t/i1}$) (36) also interacted with KB-1753 in a nucleotide-dependent manner. Interestingly, no detectable affinity was observed for the closely related $G\alpha_{oA}$ subunit nor the more divergent G-protein, $G\alpha_s$ (Figure 1C).

Overall structure of $G\alpha_{i1}$·GDP·AlF_4^-/KB-1753

To understand the molecular details of the nucleotide-dependent interaction of KB-1753 with Gα, we determined the structure of KB-1753 bound to $G\alpha_{i1}$·GDP·AlF_4^- by X-ray diffraction crystallography (Table 1). The conformation of Gα·GDP·AlF_4^- closely resembles that of Gα·GTPγS (37,38), and AlF_4^- addition activates Gα signaling *in vitro* (39). The overall structure of $G\alpha_{i1}$ consists of two principal lobes: a Ras-like domain similar to the monomeric GTPase fold and an additional all-helical domain (11); the guanine nucleotide binding pocket lies between these two domains. The planar anion AlF_4^-, GDP, and Mg^{2+} are all found in the $G\alpha_{i1}$/KB-1753 structure as predicted (Figure 2A). Three flexible 'switch' regions, responsible

for the conformational changes involved in the guanine nucleotide cycle (11), aid in the binding of AlF_4^- and Mg^{2+} (Figure 2A).

Two nearly identical $G\alpha_{i1}$/KB-1753 dimers exist in the asymmetric unit with an r.m.s.d. of 0.64 Å. Residues Arg-3 through Glu-13 of the KB-1753 peptide (S_1SRGYYHGI WVGEEGRLSR$_{19}$) were sufficiently ordered to confidently model based on electron density (Figure 2B,C). KB-1753 binds within the Ras-like domain of $G\alpha_{i1}$ in a highly conserved hydrophobic cleft formed by the α2 (switch II) and α3 helices (Figure 2). This cleft represents the proposed effector-binding site for $G\alpha_{i1}$ (40) and suggests that KB-1753 binds in an 'effector-like' mode to activated-state $G\alpha$ (see below). Notably, binding of KB-1753 does not significantly alter the conformation of $G\alpha_{i1}$ as the overall r.m.s.d. between bound and unbound structures was calculated to be 0.81 Å. Hydrophobic residues dominate the $G\alpha_{i1}$/KB-1753 binding interface, including Ile-9 of KB-1753, which lies buried within the hydrophobic pocket created by $G\alpha_{i1}$ residues Trp-211 and Phe-215. Conservative replacement of this isoleucine with valine leads to a five-fold decrease in binding affinity, whereas alanine substitution at Ile-9 (in combination with the critical Trp-10, see below) completely abolishes interaction of KB-1753 with $G\alpha_{i1}$ (Figure 3B). Additional van der Waals contacts are made between His-7 and Ile-212 within this pocket. Other KB-1753/$G\alpha_{i1}$ contacts include Val-11/Arg-208, Trp-10/ Lys-248, Trp-10/Ser-252, His-7/Asn-256, and Gly-8/Asn-256 (Figure 2B and Figure 3A).

When bound to $G\alpha_{i1}$, KB-1753 assumes a hairpin secondary structure centered about residues Tyr-6 and His-7, with several stabilizing intramolecular contacts aiding the adoption of this hairpin (*e.g.*, Figure 2B). The position of the imidazole nitrogen of His-7 raises the possibility of a cation-pi interaction with Tyr-6 at the hinge of the hairpin loop. Mutation of this histidine results in a seven-fold reduction in binding affinity ("H7F"; Figure 3C). Other intramolecular contacts within the bound conformation of KB-1753 include Gly-4/Val-11, Gly-4/Gly-12, Tyr-5/Trp-10, Tyr-6/Ile-9, Tyr-6/Val-11 (Figure 2B and Figure 3A). Figure 2C illustrates the electron density depicting the confidence of model building of KB-1753 and its interaction with $G\alpha_{i1}$.

Molecular basis of nucleotide-dependent interaction

Binding of an activating nucleotide such as GTP, GTPγS, or GDP·AlF_4^- to $G\alpha$ induces specific structural changes in the three switch regions. The conformations of these switch regions are very similar in the $G\alpha$·GDP·AlF_4^- and $G\alpha$·GTPγS forms (11), explaining the ability of KB-1753 to bind these two conformations equipotently. In these active conformations, Arg-208 in switch II makes a critical contact with Glu-245 of the α3 helix, just beyond switch III, which helps stabilize the switch II conformation (37,38). Interestingly, the indole nitrogen of Trp-10 in KB-1753 exploits this interaction and makes contacts with both Arg-208 and Glu-245 (Figure 2B). These interactions may thus partially contribute to the selective nature of KB-1753 binding to activated $G\alpha$, as switch II is entirely disordered in the structure of $G\alpha$·GDP likely due to a lack of stabilization with switch III (11). Indeed, this conserved glutamate residue makes contacts with effectors in the structures of $G\alpha_t$/PDEγ, $G\alpha_{13}$/p115-RhoGEF, and $G\alpha_q$/ GRK2 dimers, although the contributing effector residues are not tryptophan as seen here with KB-1753 (6). However, the exact degree to which this interaction aids in the nucleotide selectivity of KB-1753 cannot be inferred as Trp-10 may play other critical roles in the $G\alpha$/ KB-1753 interaction, such as stabilization of the peptide conformation.

The hydrophobic binding pocket created by Trp-211 and Phe-215 likely also contributes to the nucleotide selectivity of KB-1753. The overall architecture of this pocket perfectly accommodates the Ile-9 of KB-1753. A highly conservative replacement of Ile-9 with valine, lacking a single methyl extension, results in a loss of binding affinity ("I9V"; Figure 3C). Furthermore, given the inherent flexibility of switch II in the GDP-bound state (11), the integrity of this pocket would be compromised in the inactive conformation. Our recent

structural analysis of $G\alpha_{i1}$ bound to a GDP-selective peptide, KB-752, revealed a similar mode of interaction with the Trp-211/Phe-215 pocket (10). In the case of KB-752, however, a tryptophan from the peptide was perfectly accommodated by the Trp-211/Phe-215 hydrophobic pocket only in the inactive conformation, given that active conformations present steric clash with the larger tryptophan side chain (10). These results underscore the critical involvement of the hydrophobic pocket formed from the $\alpha2/\alpha3$ helices in binding these regulatory peptides and dictating their nucleotide selectivities.

KB-1753 blocks Gα/effector interaction

The binding site for KB-1753 on $G\alpha_{i1}$ lies in the putative effector-binding region. Mutational analyses implicate this region as the binding site on $G\alpha_{i1}$ for adenylyl cyclase (40). Moreover, crystal structures of $G\alpha_s$/adenylyl cyclase and $G\alpha_t$/PDEγ have established the $\alpha2/\alpha3$ pocket, along with the $\alpha2/\beta4$ loop, as the effector binding site for these G-protein subunits (3,4). As $G\alpha_t$ and $G\alpha_{i1}$ are members of the same Gα subfamily, we focused on the $G\alpha_t$/PDEγ interaction to validate that KB-1753 binds to the Gα effector-binding site and could thus serve as a unique effector antagonist. The $G\alpha_{i1}$/KB-1753 and $G\alpha_t$/PDEγ structures indicate similar modes of Gα interaction between these two peptides (Figure 4A). We first demonstrated using SPR that a soluble $G\alpha_{t/i1}$ chimera (containing $G\alpha_{i1}$ sequence from residues 215 [end of α2 helix] through 294 [start of α4 helix]; ref. 36) could bind both KB-1753 and a peptide comprising residues 63–87 of PDEγ (Figure 4B inset). We next tested whether KB-1753 and PDEγ exhibit mutually exclusive binding to $G\alpha_{t/i1}$. As expected, preincubation of $G\alpha_{t/i1}$ with free KB-1753 peptide inhibited (in a dose-dependent manner) binding of $G\alpha_{t/i1} \cdot GDP \cdot AlF_4^-$ to biotinylated KB-1753 immobilized on the SPR biosensor (data not shown). Preincubation with KB-1753 also abrogated binding of $G\alpha_{t/i1} \cdot GDP \cdot AlF_4^-$ to a biotinylated PDEγ peptide surface (Figure 4B). These results establish that KB-1753 competes for effector (PDEγ) binding to $G\alpha_{t/i1}$, suggesting that KB-1753 could serve as an effector antagonist in the transducin/PDE signaling pathway.

We thus tested whether KB-1753 could perturb wildtype $G\alpha_t$ interaction with, and signaling to, cGMP phosphodiesterase (PDE6) by reconstituting these proteins with photoreceptor membranes containing light-activatable rhodopsin, the receptor upstream of transducin. As part of the phototransduction signaling pathway, $G\alpha_t \cdot GTP$ activates PDE6 by binding directly to PDEγ and releasing the inhibitory constraint which PDEγ imposes on the α and β catalytic subunits of PDE6 (41).We tested whether KB-1753 could impair PDE6 activation by $G\alpha_t \cdot GTP$ by measuring the steady-state rate of cGMP degradation to GMP. Rhodopsin-activated transducin was observed to stimulate degradation of cGMP in reconstituted ROS membranes (Figure 4C). KB-1753, but not the I9A/W10Asubstituted peptide, nearly abolished the stimulation of PDE6 cGMP hydrolysis activity (Figure 4C). Together, the results from SPR competition binding and PDE6 activity assays confirm the ability of KB-1753 to interdict GPCR-mediated signaling through activated G-proteins to effector enzyme activity and suggest that KB-1753 could serve as a novel tool for antagonizing these signaling pathways.

KB-1753 interferes with RGS protein GAP activity

We also reasoned that, by binding to the transition-state mimetic form of Gα ($G\alpha \cdot GDP \cdot AlF_4^-$), KB-1753 may alter the intrinsic and/or RGS protein-stimulated GTPase activity of $G\alpha_t$ and $G\alpha_{i1}$. The experiments conducted with wildtype $G\alpha_t$ reconstituted with photoreceptor membranes revealed the presence of both effects (Figure 5A). Addition of KB-1753 caused a nearly 2-fold increase in the basal rate of $G\alpha_t$ GTPase activity. This activity may arise from stabilization of switch II by KB-1753 in a conformation suitable for the catalytic Gln-204 of Gα to more efficiently participate in GTP hydrolysis. Addition of KB-1753 also caused an ~40% reversal of GTPase acceleration by an RGS protein, RGS16, previously shown to act on $G\alpha_t$ (42). Neither effect was observed with control I9A/W10A-substituted peptide.

Partial inhibition of RGS16 GAP activity by KB-1753 was very similar to well-documented partial inhibition caused by PDEγ (lowest bar in Figure 5A; see refs. (43, 44) for original observation).

Comparing the Gα/KB-1753 and Gα/RGS4 structures reveals no significant alterations in the overall Gα backbone (r.m.s.d. of 0.68 Å) nor of the critical catalytic residues R178, T181, and Q204. However, space-filling models of KB-1753 and RGS4 indicate that, although KB-1753 binds to the effector-binding region of Gα, which is exclusive from the RGS protein-binding interface (5,6), the C-terminus of KB-1753 could sterically hinder RGS protein access to its Gα binding site (Figure 5B). KB-1753 significantly blocked the GAP activity of RGS12 on Gα$_{i1}$ (Figure 5C,D), suggesting that KB-1753 interferes with RGS protein binding. We also observed a small peptide-dependent acceleration of basal Gα$_{i1}$ GTPase activity (Figure 5C) although, unlike in the case of wildtype Gα$_t$ (Figure 5A), this effect was not statistically significant. Using a fluorescence resonance energy transfer (FRET)-based assay for Gα/RGS protein interactions (34), we confirmed that KB-1753 is able to block the direct interaction between RGS4 and Gα$_{i1}$ (Figure 5E). Thus, KB-1753 serves as a novel peptide inhibitor of Gα$_{i1}$/RGS protein interaction and RGS-mediated GAP activity *in vitro*.

A fusion of KB-1753 onto yellow fluorescent protein serves as a sensor for activated Gα

Fluorescent biosensors have become instrumental for investigating protein-protein interactions as well as protein activation in real-time and visualizing the spatiotemporal aspects of signal transduction in live cells (45,46). The ability of KB-1753 to bind only activated Gα makes it a potentially useful tool for developing novel biosensors for G-protein activation. In an initial test of this hypothesis, we employed FRET between chromatic variants of the *Aequoria victoria* green fluorescent protein in which excitation of a donor cyan fluorescent protein (CFP) in turn excites an acceptor yellow fluorescent protein (YFP) when these variants are within defined distance constraints (~50 Å) (47). We subcloned the KB-1753 peptide sequence N-terminal to YFP (KB-1753-YFP) to serve as a FRET acceptor for CFP-modified Gα$_{i1}$ (Figure 5B; ref. 34). KB-1753-YFP underwent a robust FRET response with CFP-Gα$_{i1}$, selectively in the presence of aluminum tetrafluoride (Figure 6A, B) and with an affinity of ~750 nM (Figure 6C). Incubation of CFP-Gα$_{i1}$ with excess unmodified KB-1753 (but not the I9A/W10A mutant) blocked the FRET response (Figure 6B). These results validate KB-1753-YFP as a *bona fide* FRET partner for detecting the activated conformation of CFP-tagged Gα$_{i1}$ – a form of KB-1753 that could be directly applied to *in vivo* settings (45,46).

DISCUSSION

The structural basis of G-protein regulation resides in subtle conformational changes in three critical switch regions of the Gα subunit (11). Upon GDP release from the inactive, Gβγ-complexed conformation, Gα binds GTP and adopts the active conformation capable of regulating effector molecules. Regulatory proteins (such as RGS proteins and GoLoco proteins) exploit these distinct nucleotide-dependent conformations of Gα for their binding and modulation of the nucleotide cycle (7,8,48). Here, we have described a peptide, KB-1753, capable of interacting with specific Gα subunits solely in active conformations. The crystal structure of this peptide bound to Gα$_{i1}$·GDP·AlF$_4^-$ reveals an 'effector-like' mode of binding, relying on the specific conformation of the switch II helix. KB-1753 serves as an effector antagonist as well as an inhibitor of RGS protein activity. These qualities make KB-1753 an attractive new tool for studying G-protein signaling. The development of biosensors for activated Gα using KB-1753 should open new avenues for both *in vitro* assay design and real-time *in vivo* imaging of Gα activation.

Currently, available Gα/effector structures include Gα$_s$/adenylyl cyclase, Gα$_q$/GRK2, Gα$_{13}$/p115RhoGEF, and Gα$_t$/PDEγ/RGS9 (3–6). Although Gα$_t$ belongs to the Gα$_i$ family, currently

no specific structural analysis of a $G\alpha_{i1-3}$/effector complex exists. Thus, the $G\alpha_{i1}$/KB-1753 complex represents the first structural glimpse of $G\alpha_{i1}$ engaged in an effector-like recognition mode, albeit with a nonphysiological target. Based on the $G\alpha_s$/adenylyl cyclase structure and the pseudosymmetry of the C1 and C2 cytosolic lobes of adenylyl cyclase (3), mutational analysis has revealed residues within the C1 lobe of type V adenylyl cyclase (ACV) critical to $G\alpha_{i1}$ regulation (49). Specifically, these critical C1 lobe residues reside in the $\alpha1/\alpha2$ and the $\alpha3/\beta4$ segments of ACV, with the latter segment proposed to bind within the switch II/$\alpha3$ cleft of $G\alpha_i$, the binding site for KB-1753. However, no significant sequence similarity was observed between KB-1753 and the $\alpha3/\beta4$ loop of ACV. A sequence of S**L**VRE**M**TGVNV within the ACV $\alpha3/\beta4$ loop has been implicated in binding the switch II/$\alpha3$ cleft of $G\alpha_i$; bolded, underlined residues indicate particular positions that, when mutated, result in loss of $G\alpha_i$-mediated inhibition (49). Aside from a general hydrophobic character in this region of ACV that may complement the hydrophobic cleft in $G\alpha$, no significant homology exists with KB-1753. Thus, KB-1753 appears to be a unique sequence that exploits the same effector-binding region of $G\alpha_{i1}$, and suggests that diverse primary sequences in effectors may recognize a similar binding motif within $G\alpha$. Indeed, the switch II/$\alpha3$ cleft utilized by effectors is highly conserved among $G\alpha$ subfamilies (Figure 7) (3–6); therefore, diversity within effectors, either in primary sequence or tertiary structure, must compensate for the common $G\alpha$ binding groove to allow for signaling specificity (6). This difficulty in defining $G\alpha$/effector specificity based on the conserved nature of structurally-defined interactions has been previously discussed (6). Another possibility is that additional regions of $G\alpha$ define effector specificity by complementing the conserved interactions within the switch II/$\alpha3$ cleft. For example, regions within the $\alpha4/\beta6$ loop of $G\alpha_{i2}$ (specifically [314]RKDTKE[319]) have been implicated in the interaction with adenylyl cyclase (40). However, KB-1753 makes no contact within this region of $G\alpha$. Also, the $\alpha2/\beta4$ and $\alpha3/\beta5$ regions of $G\alpha$ have been implicated in effector binding; however, with the exception of $G\alpha_s$, these sequences are also highly conserved (6). The ability of KB-1753 to inhibit binding and signaling of wildtype transducin to PDE6, an effector to which KB-1753 also lacks significant sequence similarity, signifies its effector-like mode of binding to $G\alpha_{i1}$ and further underscores the sequence diversity in effectors available for $G\alpha$ subunit recognition.

KB-1753 is a potentially attractive new tool for studying G-protein signaling. If modified to allow cell penetration (e.g., ref. 50), KB-1753 could effectively block $G\alpha_i$·GTP/effector signaling while preserving receptor/heterotrimer coupling and $G\beta\gamma$-mediated signaling, unlike pertussis toxin which permanently impairs $G\alpha_i\beta\gamma$ coupling and signaling via ADP-ribosylation (51) or of siRNA-mediated *Gnai* transcript silencing which can result in compensatory upregulation of other $G\alpha_{i/o}$ family members (52). The selective interaction of KB-1753 with $G\alpha_i$ subunits over $G\alpha_o$ (Fig. 1B) would provide another advantage in interrogating GPCR coupling specificity over pertussis toxin, the latter acting nonspecifically on all $G\alpha_{i/o}$ subfamily members except $G\alpha_z$ (53). The ability of KB-1753 to block RGS protein binding and resultant GAP activity highlights yet another potential usefulness of this novel peptide.

Biosensors capable of visualizing the spatiotemporal aspects of protein activation and protein-protein interactions have become indispensable tools for studying signal transduction events within the context of live cells (47,54). Several studies using CFP/YFP FRET and related techniques have investigated GPCR signaling dynamics (55–58). Studies interrogating heterotrimer activation have used designs wherein activation leads to a *reduction* in FRET response due to the dissociation of a $G\alpha$-CFP and $G\beta\gamma$-YFP coupled pair, for example, ref. (57). Although innovative and informative, these studies are limited by their reliance on a *loss* of FRET response which presents specific technical challenges (such as correcting for photobleaching artifacts) and limits the ability to track the spatiotemporal aspects of $G\alpha$ signaling once activated. Our KB-1753-YFP, however, presents an attractive alternative design that produces an *increase* in FRET response following $G\alpha$ activation (Figure 6) and should

allow resolution of the spatiotemporal dynamics of activated Gα signaling. Moreover, as Gα becomes deactivated, a loss of FRET response would be expected, given that KB-1753-YFP binds selectively to only the activated form. Thus, a FRET-based approach with KB-1753-YFP could report both the activation and deactivation dynamics of Gα signaling potentially improving the resolution of previous studies. We are now avidly working towards this goal.

ACKNOWLEDGMENTS

REFERENCES

1. McCudden CR, Hains MD, Kimple RJ, Siderovski DP, Willard FS. G-protein signaling: back to the future. Cell Mol Life Sci 2005;62:551–577. [PubMed: 15747061]

2. Wettschureck N, Offermanns S. Mammalian G proteins and their cell type specific functions. Physiol Rev 2005;85:1159–1204. [PubMed: 16183910]

3. Tesmer JJ, Sunahara RK, Gilman AG, Sprang SR. Crystal structure of the catalytic domains of adenylyl cyclase in a complex with Gsalpha.GTPgammaS. Science 1997;278:1907–1916. [PubMed: 9417641]

4. Slep KC, Kercher MA, He W, Cowan CW, Wensel TG, Sigler PB. Structural determinants for regulation of phosphodiesterase by a G protein at 2.0 A. Nature 2001;409:1071–1077. [PubMed: 11234020]

5. Chen Z, Singer WD, Sternweis PC, Sprang SR. Structure of the p115RhoGEF rgRGS domain-Galpha13/i1 chimera complex suggests convergent evolution of a GTPase activator. Nat Struct Mol Biol 2005;12:191–197. [PubMed: 15665872]

6. Tesmer VM, Kawano T, Shankaranarayanan A, Kozasa T, Tesmer JJ. Snapshot of activated G proteins at the membrane: the Galphaq-GRK2-Gbetagamma complex. Science 2005;310:1686–1690. [PubMed: 16339447]

7. Ross EM, Wilkie TM. GTPase-activating proteins for heterotrimeric G proteins: regulators of G protein signaling (RGS) and RGS-like proteins. Annu Rev Biochem 2000;69:795–827. [PubMed: 10966476]

8. Siderovski DP, Willard FS. The GAPs, GEFs, and GDIs of heterotrimeric G-protein alpha subunits. Int J Biol Sci 2005;1:51–66. [PubMed: 15951850]

9. Johnston CA, Ramer JK, Blaesius R, Fredericks Z, Watts VJ, Siderovski DP. A bifunctional Galphai/Galphas modulatory peptide that attenuates adenylyl cyclase activity. FEBS Lett 2005;579:5746–5750. [PubMed: 16225870]

10. Johnston CA, Willard FS, Jezyk MR, Fredericks Z, Bodor ET, Jones MB, Blaesius R, Watts VJ, Harden TK, Sondek J, Ramer JK, Siderovski DP. Structure of Galpha(i1) bound to a GDP-selective peptide provides insight into guanine nucleotide exchange. Structure 2005;13:1069–1080. [PubMed: 16004878]

11. Sprang SR. G protein mechanisms: insights from structural analysis. Annu Rev Biochem 1997;66:639–678. [PubMed: 9242920]

12. Hamm HE. How activated receptors couple to G proteins. Proc Natl Acad Sci U S A 2001;98:4819–4821. [PubMed: 11320227]

13. Meng EC, Bourne HR. Receptor activation: what does the rhodopsin structure tell us? Trends Pharmacol Sci 2001;22:587–593. [PubMed: 11698103]

14. Rondard P, Iiri T, Srinivasan S, Meng E, Fujita T, Bourne HR. Mutant G protein alpha subunit activated by Gbeta gamma: a model for receptor activation? Proc Natl Acad Sci U S A 2001;98:6150–6155. [PubMed: 11344266]

15. Davis TL, Bonacci TM, Sprang SR, Smrcka AV. Structural and molecular characterization of a preferred protein interaction surface on G protein beta gamma subunits. Biochemistry 2005;44:10593–10604. [PubMed: 16060668]

16. Hessling J, Lohse MJ, Klotz KN. Peptide G protein agonists from a phage display library. Biochem Pharmacol 2003;65:961–967. [PubMed: 12623127]

17. Ja WW, Roberts RW. In vitro selection of state-specific peptide modulators of G protein signaling using mRNA display. Biochemistry 2004;43:9265–9275. [PubMed: 15248784]

18. Scott JK, Huang SF, Gangadhar BP, Samoriski GM, Clapp P, Gross RA, Taussig R, Smrcka AV. Evidence that a protein-protein interaction 'hot spot' on heterotrimeric G protein betagamma subunits is used for recognition of a subclass of effectors. Embo J 2001;20:767–776. [PubMed: 11179221]

19. Stols L, Gu M, Dieckman L, Raffen R, Collart FR, Donnelly MI. A new vector for high-throughput, ligation-independent cloning encoding a tobacco etch virus protease cleavage site. Protein Expr Purif 2002;25:8–15. [PubMed: 12071693]

20. Kimple RJ, Willard FS, Hains MD, Jones MB, Nweke GK, Siderovski DP. Guanine nucleotide dissociation inhibitor activity of the triple GoLoco motif protein G18: alanine-to-aspartate mutation restores function to an inactive second GoLoco motif. Biochem J 2004;378:801–808. [PubMed: 14656218]

21. McCudden CR, Willard FS, Kimple RJ, Johnston CA, Hains MD, Jones MB, Siderovski DP. G alpha selectivity and inhibitor function of the multiple GoLoco motif protein GPSM2/LGN. Biochim Biophys Acta 2005;1745:254–264. [PubMed: 15946753]

22. Snow BE, Antonio L, Suggs S, Siderovski DP. Cloning of a retinally abundant regulator of G-protein signaling (RGS-r/RGS16): genomic structure and chromosomal localization of the human gene. Gene 1998;206:247–253. [PubMed: 9469939]

23. Arshavsky VY, Dumke CL, Zhu Y, Artemyev NO, Skiba NP, Hamm HE, Bownds MD. Regulation of transducin GTPase activity in bovine rod outer segments. J Biol Chem 1994;269:19882–19887. [PubMed: 8051070]

24. Nekrasova ER, Berman DM, Rustandi RR, Hamm HE, Gilman AG, Arshavsky VY. Activation of transducin guanosine triphosphatase by two proteins of the RGS family. Biochemistry 1997;36:7638–7643. [PubMed: 9201904]

25. Snow BE, Brothers GM, Siderovski DP. Molecular cloning of regulators of G-protein signaling family members and characterization of binding specificity of RGS12 PDZ domain. Methods Enzymol 2002;344:740–761. [PubMed: 11771424]

26. Otwinowski Z, Minor W. Processing of X-ray diffraction data collected in oscillation mode. Methods Enzymol 1997;276:307–326.

27. Navaza J. Implementation of molecular replacement in AMoRe. Acta Crystallogr D Biol Crystallogr 2001;57:1367–1372. [PubMed: 11567147]

28. Jones TA, Zou JY, Cowan SW, Kjeldgaard M. Improved methods for building protein models in electron density maps and the location of errors in these models. Acta Crystallogr A 1991;47(Pt 2): 110–119. [PubMed: 2025413]

29. Brunger AT, Adams PD, Clore GM, DeLano WL, Gros P, Grosse-Kunstleve RW, Jiang JS, Kuszewski J, Nilges M, Pannu NS, Read RJ, Rice LM, Simonson T, Warren GL. Crystallography & NMR system: A new software suite for macromolecular structure determination. Acta Crystallogr D Biol Crystallogr 1998;54(Pt 5):905–921. [PubMed: 9757107]

30. Artemyev NO, Arshavsky VY, Cote RH. Photoreceptor phosphodiesterase: interaction of inhibitory gamma subunit and cyclic GMP with specific binding sites on catalytic subunits. Methods 1998;14:93–104. [PubMed: 9500861]

31. Ross EM. Quantitative assays for GTPase-activating proteins. Methods Enzymol 2002;344:601–617. [PubMed: 11771414]

32. Martemyanov KA, Arshavsky VY. Kinetic approaches to study the function of RGS9 isoforms. Methods Enzymol 2004;390:196–209. [PubMed: 15488179]

33. Skiba NP, Hopp JA, Arshavsky VY. The effector enzyme regulates the duration of G protein signaling in vertebrate photoreceptors by increasing the affinity between transducin and RGS protein. J Biol Chem 2000;275:32716–32720. [PubMed: 10973941]

34. Willard FS, Kimple RJ, Kimple AJ, Johnston CA, Siderovski DP. Fluorescence-based assays for RGS box function. Methods Enzymol 2004;389:56–71. [PubMed: 15313559]

35. Gasteiger E, Jung E, Bairoch A. SWISS-PROT: connecting biomolecular knowledge via a protein database. Curr Issues Mol Biol 2001;3:47–55. [PubMed: 11488411]

36. Pereira R, Cerione RA. A switch 3 point mutation in the alpha subunit of transducin yields a unique dominant-negative inhibitor. J Biol Chem 2005;280:35696–35703. [PubMed: 16103122]

37. Coleman DE, Berghuis AM, Lee E, Linder ME, Gilman AG, Sprang SR. Structures of active conformations of Gi alpha 1 and the mechanism of GTP hydrolysis. Science 1994;265:1405–1412. [PubMed: 8073283]

38. Sondek J, Lambright DG, Noel JP, Hamm HE, Sigler PB. GTPase mechanism of Gproteins from the 1.7-A crystal structure of transducin alpha-GDP-AIF-4. Nature 1994;372:276–279. [PubMed: 7969474]

39. Sternweis PC, Gilman AG. Aluminum: a requirement for activation of the regulatory component of adenylate cyclase by fluoride. Proc Natl Acad Sci U S A 1982;79:4888–4891. [PubMed: 6289322]

40. Grishina G, Berlot CH. Identification of common and distinct residues involved in the interaction of alphai2 and alphas with adenylyl cyclase. J Biol Chem 1997;272:20619–20626. [PubMed: 9252377]

41. Arshavsky VY, Lamb TD, Pugh EN Jr. G proteins and phototransduction. Annu Rev Physiol 2002;64:153–187. [PubMed: 11826267]

42. Chen CK, Wieland T, Simon MI. RGS-r, a retinal specific RGS protein, binds an intermediate conformation of transducin and enhances recycling. Proc Natl Acad Sci U S A 1996;93:12885–12889. [PubMed: 8917514]

43. Natochin M, Granovsky AE, Artemyev NO. Regulation of transducin GTPase activity by human retinal RGS. J Biol Chem 1997;272:17444–17449. [PubMed: 9211888]

44. Wieland T, Chen CK, Simon MI. The retinal specific protein RGS-r competes with the gamma subunit of cGMP phosphodiesterase for the alpha subunit of transducin and facilitates signal termination. J Biol Chem 1997;272:8853–8856. [PubMed: 9083000]

45. Hahn K, Toutchkine A. Live-cell fluorescent biosensors for activated signaling proteins. Curr Opin Cell Biol 2002;14:167–172. [PubMed: 11891115]

46. Johnston CA, Siderovski DP. Resolving G protein-coupled receptor signaling mechanics in vivo using fluorescent biosensors. Cellscience Reviews 2006;2:16–24.

47. Zhang J, Campbell RE, Ting AY, Tsien RY. Creating new fluorescent probes for cell biology. Nat Rev Mol Cell Biol 2002;3:906–918. [PubMed: 12461557]

48. Willard FS, Kimple RJ, Siderovski DP. Return of the GDI: the GoLoco motif in cell division. Annu Rev Biochem 2004;73:925–951. [PubMed: 15189163]

49. Dessauer CW, Tesmer JJ, Sprang SR, Gilman AG. Identification of a Gialpha binding site on type V adenylyl cyclase. J Biol Chem 1998;273:25831–25839. [PubMed: 9748257]

50. Lindsay MA. Peptide-mediated cell delivery: application in protein target validation. Curr Opin Pharmacol 2002;2:587–594. [PubMed: 12324264]

51. Katada T, Bokoch GM, Smigel MD, Ui M, Gilman AG. The inhibitory guanine nucleotide-binding regulatory component of adenylate cyclase. Subunit dissociation and the inhibition of adenylate cyclase in S49 lymphoma cyc- and wild type membranes. J Biol Chem 1984;259:3586–3595. [PubMed: 6142891]

52. Krumins AM, Gilman AG. Targeted knockdown of G protein subunits selectively prevents receptor-mediated modulation of effectors and reveals complex changes in nontargeted signaling proteins. J Biol Chem. 2006

53. Fields TA, Casey PJ. Signalling functions and biochemical properties of pertussis toxin-resistant G-proteins. Biochem J 1997;321(Pt 3):561–571. [PubMed: 9032437]

54. Chamberlain C, Hahn KM. Watching proteins in the wild: fluorescence methods to study protein dynamics in living cells. Traffic 1 2000:755–762.

55. Bunemann M, Frank M, Lohse MJ. Gi protein activation in intact cells involves subunit rearrangement rather than dissociation. Proc Natl Acad Sci U S A 2003;100:16077–16082. [PubMed: 14673086]

56. Hein P, Frank M, Hoffmann C, Lohse MJ, Bunemann M. Dynamics of receptor/G protein coupling in living cells. Embo J 2005;24:4106–4114. [PubMed: 16292347]

57. Janetopoulos C, Jin T, Devreotes P. Receptor-mediated activation of heterotrimeric G-proteins in living cells. Science 2001;291:2408–2411. [PubMed: 11264536]

58. Vilardaga JP, Bunemann M, Krasel C, Castro M, Lohse MJ. Measurement of the millisecond activation switch of G protein-coupled receptors in living cells. Nat Biotechnol 2003;21:807–812. [PubMed: 12808462]

59. Aiyar A. The use of CLUSTAL W and CLUSTAL X for multiple sequence alignment. Methods Mol Biol 2000;132:221–241. [PubMed: 10547838]
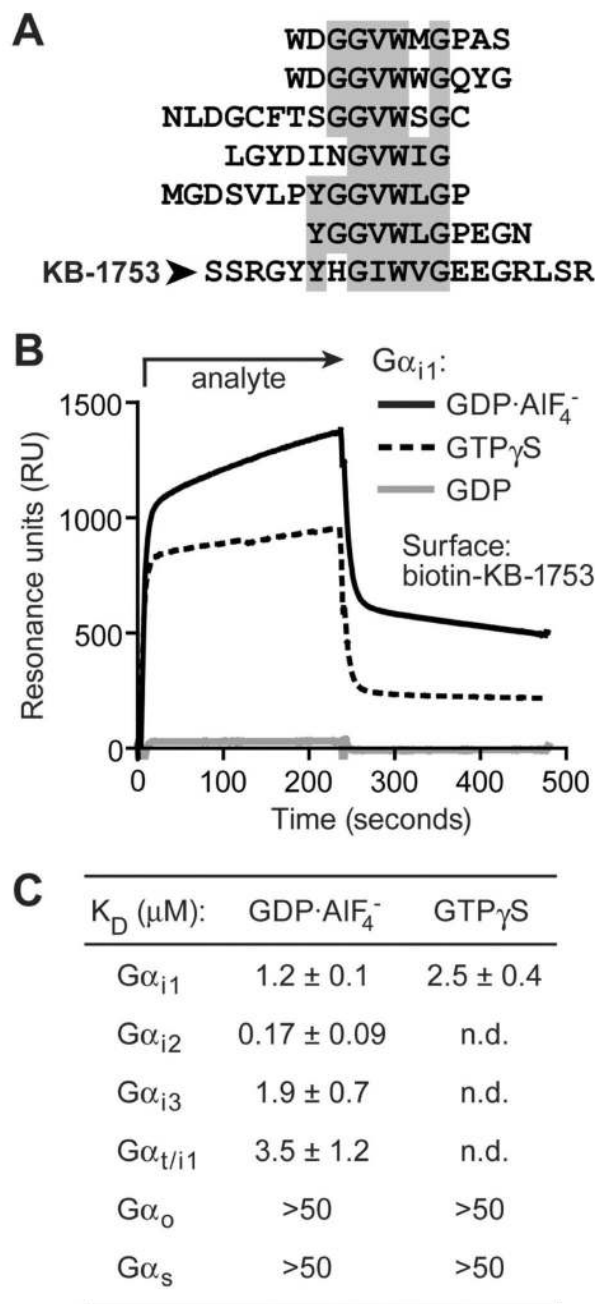
Figure 1. Selective binding of KB-1753 to Gα subunits as measured by surface plasmon resonance (SPR)

(**A**) Sequences of seven peptides, including KB-1753, with a shared sequence (grey) isolated by phage-display based on selective binding to immobilized $G\alpha_{i1} \cdot GTP\gamma S$ (10). (**B**) 10 µM $G\alpha_{i1}$ protein ("analyte"), in each of three nucleotide-bound states as indicated, was injected over immobilized, biotinylated KB-1753 peptide. Non-specific binding (~200 RU) to a control peptide surface was subtracted from each curve. (**C**) Indicated Gα subunits, including a chimera between $G\alpha_{transducin}$ and $G\alpha_{i1}$ ("$G\alpha_{t/i1}$"), were separately injected at increasing concentrations (0.01 – 50 µM) over immobilized KB-1753 to determine dissociation constants (K_D) for each interaction pair as obtained by saturation binding analysis (20,21). No binding ($K_D > 1000$

µM) was seen with any G α in the GDP-bound state. "$K_D > 50\,\mu M$" denotes interactions with minimal binding responses observed only at saturating concentrations of Gα greater than 50 µM. n.d., not determined.
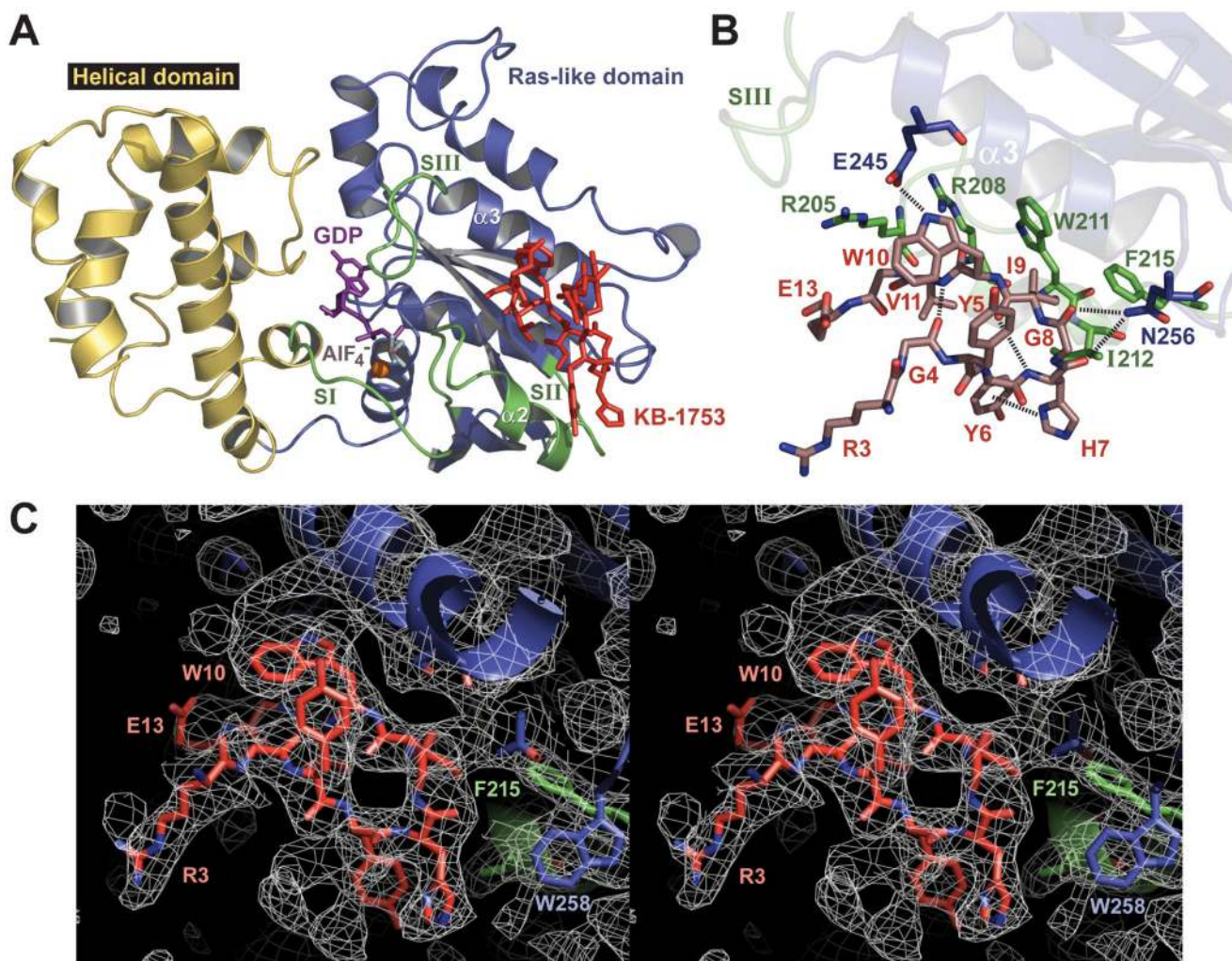
Figure 2. Structural features of the Gα$_{i1}$/KB-1753 interaction
(**A**) KB-1753 peptide (red, with side-chains) is bound between the α2 ("switch II") and α3 helices of the Gα$_{i1}$ Ras-like domain (blue; switch regions in green). No contact is made between KB-1753 and the all-helical domain (yellow), GDP (magenta), AlF$_4^-$ (grey), or magnesium (orange). (**B**) Representative inter- and intramolecular contacts between Gα$_{i1}$ (blue; switch regions in green) and KB-1753 (tan) residues are shown in black dotted lines. All contacts shown or discussed in the text were selected based on a maximum distance cutoff of 3.7 Å. (**C**) Stereoview of experimental electron density for KB-1753 bound to Gα$_{i1}$, shown as a 2F$_o$-F$_c$ simulated annealing composite omit map generated with 5% overall model omitted and contoured at 1 σ (electron density shown in white cage). The region highlighted is the entire peptide density (model in red) lying below the α3 helix (model in blue) and above switch II (model in green).
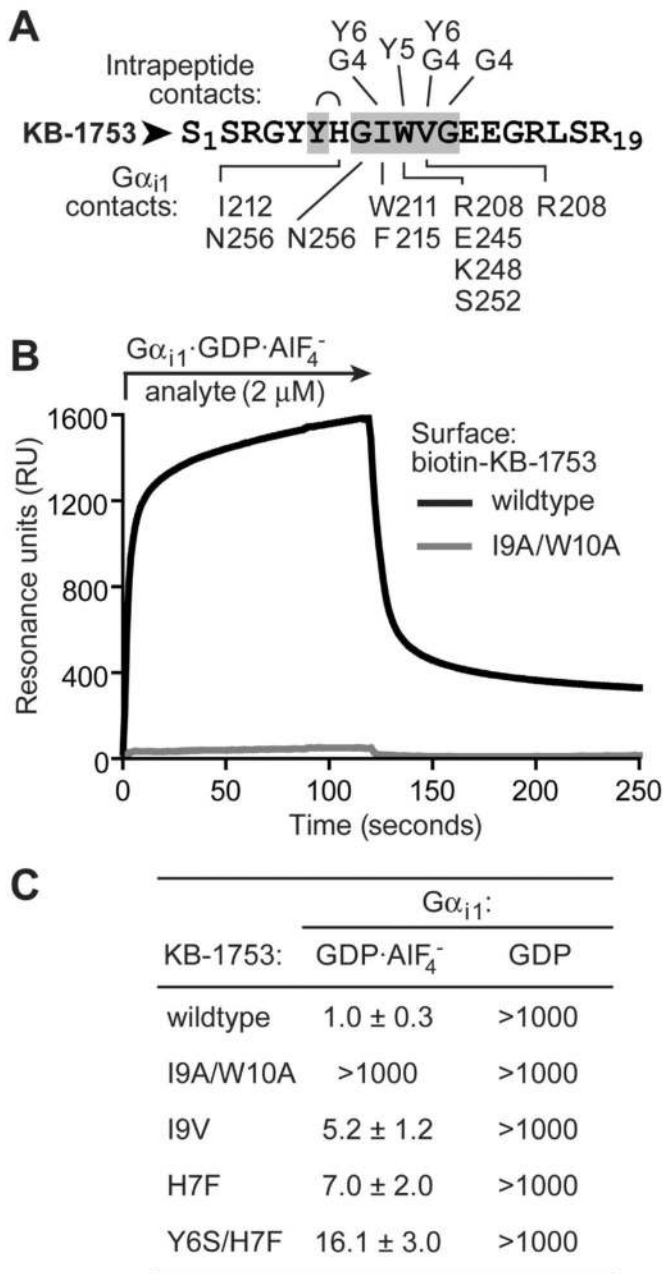
Figure 3. Effects of amino-acid substitutions on KB-1753 binding affinity
(**A**) Summary of intrapeptide and $G\alpha_{i1}$ contacts made by KB-1753 peptide residues. (**B**) N-terminally biotinylated KB-1753 peptides, either with wildtype sequence or mutated (Ile-9 and Trp-10 replaced with alanine), were immobilized on separate streptavidin-coated flow cells and 2 μM of $G\alpha_{i1} \cdot GDP \cdot AlF_4^-$ protein ("analyte") was injected over both surfaces. Non-specific binding to a control peptide was subtracted from each curve. (**C**) Dissociation constants (K_D in μM) for the interaction between $G\alpha_{i1}$, in indicated nucleotide state, and wildtype or mutant KB-1753 peptides immobilized on SPR surfaces. Other parameters are described in Figure 1C.
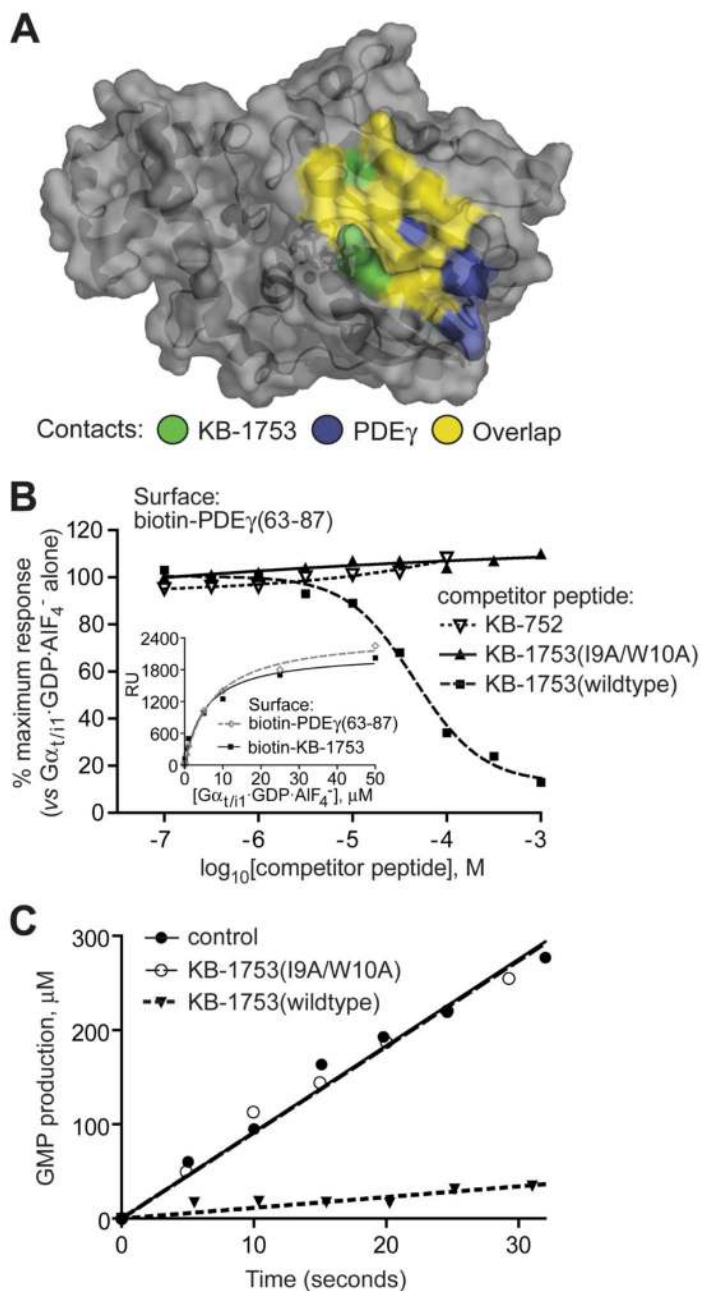
Figure 4. KB-1753 acts as an effector antagonist

(**A**) Surface rendering of $G\alpha_{i1} \cdot GDP \cdot AlF_4^-$ (grey) with contact points highlighted for KB-1753 alone (green), PDEγ alone (blue), or shared between both interactors (yellow). (**B**) Wildtype KB-1753 competes with PDEγ for binding to Gα, but not the I9A/W10A mutant peptide nor the $G\alpha_{i1} \cdot GDP$-selective peptide KB-752. AlF_4^--activated $G\alpha_{t/i1}$ protein (8.5 µM) was pre-incubated with indicated concentrations of competitor peptide prior to injection over a streptavidin SPR surface bearing biotinylated PDEγ(63–87). Inset: SPR surfaces coated with either biotinylated KB-1753 or PDEγ peptide bind with equivalent affinity to the $G\alpha_{t/i1}$ chimera bound to GDP and AlF_4^-. (**C**) Rates of cGMP hydrolysis to GMP by transducin-activated PDE6 (0.05 µM) in the absence (control) or presence of 20 µM wild type or mutant KB-1753

peptides were calculated from linear fits of the data: control = 9.2 µM GMP produced per second; wild type KB-1753 = 1.1 µM/second; I9A/W10A mutant KB-1753 = 9.1 µM/second. The data are taken from one of three similar experiments.
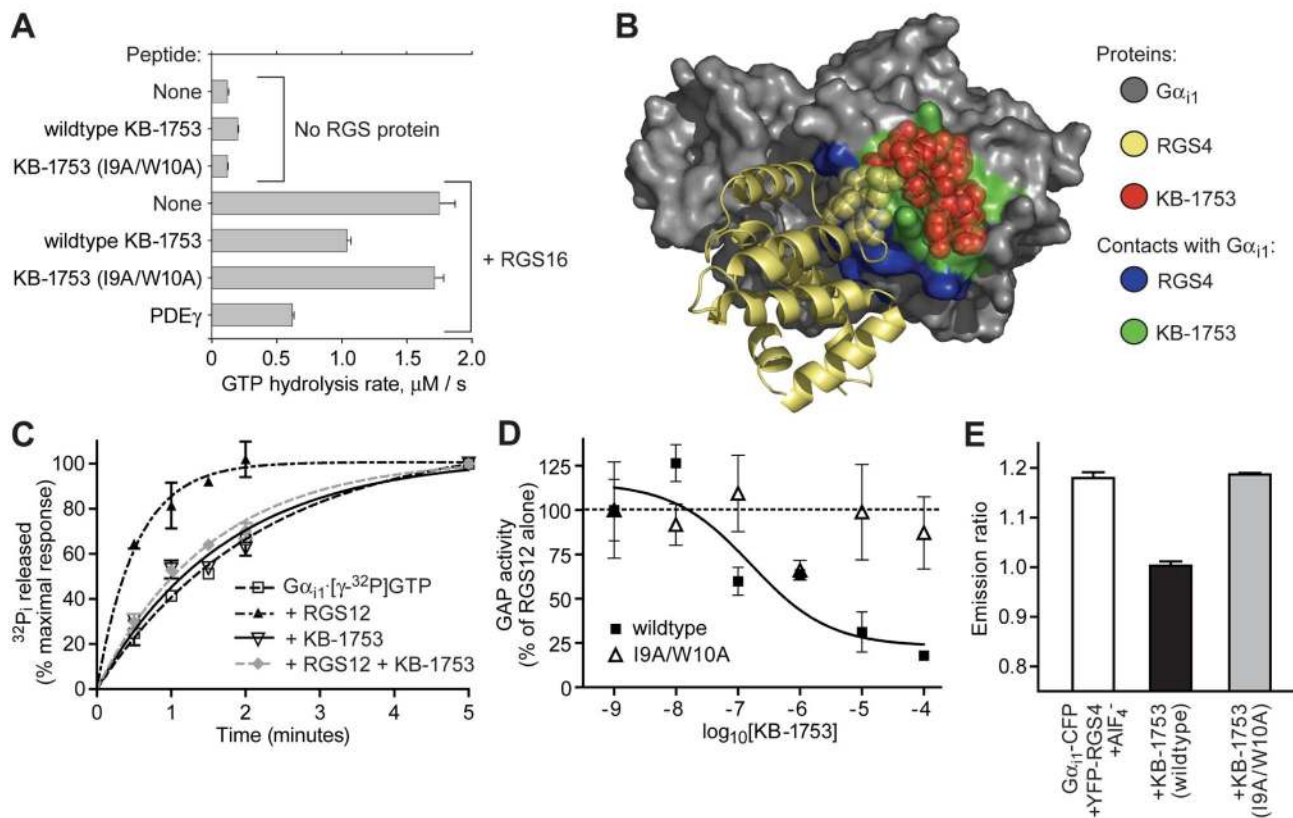
Figure 5. KB-1753 interferes with the RGS domain/Gα interaction and RGS -mediated GAP activity

(**A**) Steady-state rates of GTP hydrolysis by rhodopsin-activated transducin (1 µM) were measured in the absence or presence of 1 µM RGS16 protein, 25 µM PDEγ(63–87), and/or 20 µM wild type or mutant KB-1753 peptide, as indicated. GTP hydrolysis rates were determined from linear fits of reaction time courses; the data are averaged from two similar experiments with error bars representing SEM. (**B**) Surface rendering of $G\alpha_{i1} \cdot GDP \cdot AlF_4^-$ (grey) bound to RGS4 (cream; derived from PDB ID 1AGR) and overlaid with a space-filling representation of KB-1753 (red). Note that contacts made to $G\alpha_{i1}.GDP \cdot AlF_4^-$ by RGS4 (blue) and by KB-1753 (green) are not overlapping, yet steric hindrance is predicted between bound KB-1753 and the α5/α6 loop of RGS4 (aa 120–123 shown in space-fill). (**C**) Single-turnover GTP hydrolysis assay using [γ-^{32}P]GTP-labelled $G\alpha_{i1}$ (0.1 µM) in the absence or presence of either 0.1 µM RGS12 RGS domain or 1 µM KB-1753 or both. (**D**) Dose dependence of wildtype KB-1753-mediated inhibition of RGS12 RGS domain GAP activity, as measured in single-turnover GTPase assays performed as in panel B. The I9A/W10A mutant KB-1753 shows no inhibitory activity. (**E**) Effect of 2 µM KB-1753 peptide (wildtype or I9A/W10A mutant) on AlF_4^--dependent FRET between 0.2 µM $G\alpha_{i1}$-CFP and 0.2 µM YFP-RGS4 fusion proteins; FRET was quantified by the emission ratio (525 nm/474 nm), representing the ratio between YFP emission and CFP emission maxima upon excitation at 433 nm.
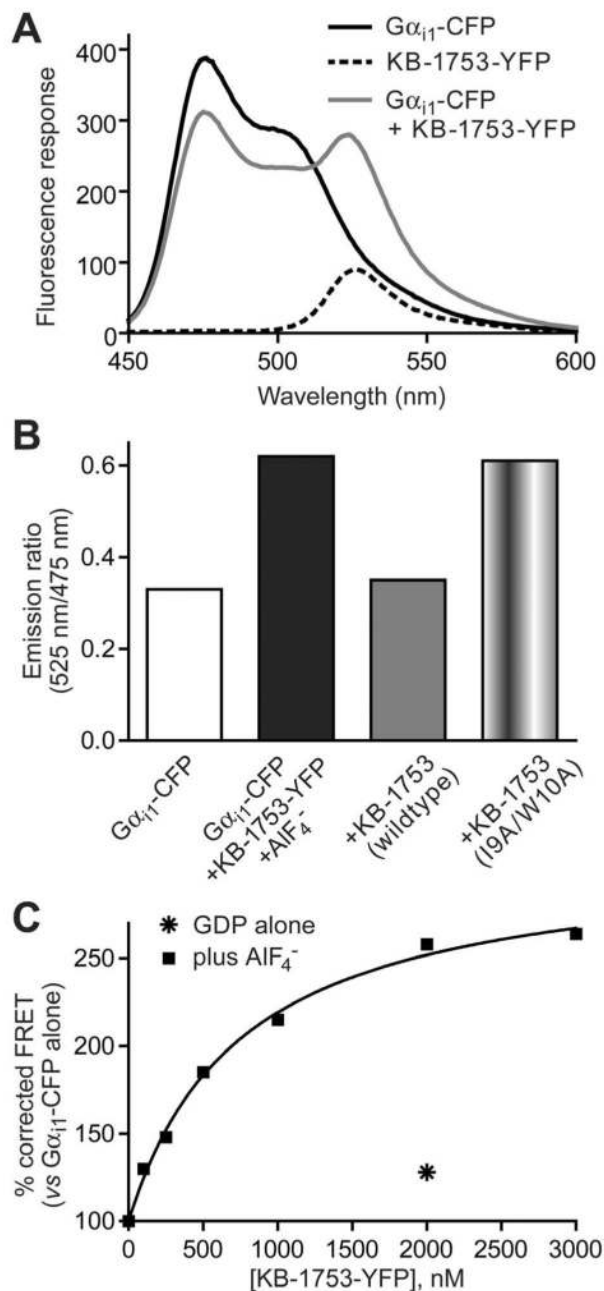
Figure 6. A KB-1753/yellow fluorescent protein fusion acts as a sensor for activated Gα$_{i1}$
(**A**) 200 nM of Gα$_{i1}$-CFP and/or 500 nM of KB-1753-YFP fusion proteins were added to cuvettes containing assay buffer (10 mM Tris, pH 7.5, 1 mM EDTA, 10 mM MgCl$_2$, 150 mM NaCl, 10 µM GDP, 30 µM AlCl$_3$, and 10 mM NaF; the latter two reagents forming the Gα activator aluminum tetrafluoride) and allowed to incubate for 60 seconds before emission scans (450 – 600 nm) were taken using an excitation wavelength of 433 nm at 20 nm/minute and slit widths of 5 nm. Data shown are uncorrected fluorescence measurements under each indicated condition. (**B**) FRET between 0.5 µM KB-1753-YFP and 0.2 µM Gα$_{i1}$·GDP·AlF$_4^-$-CFP is inhibited by pre-incubation of Gα with 2 µM wildtype KB-1753 peptide; preincubation with 2 µM of the I9A/W10A mutant was observed to have no effect on the emission ratio. (**C**) Dose-

and nucleotide-state-dependent FRET between 0.2 μM $G\alpha_{i1}$-CFP and indicated concentrations of KB-1753-YFP fusion. Data are expressed as "corrected FRET" obtained by subtracting the emission of KB-1753-YFP alone from each FRET condition. Apparent dissociation constant obtained for the KB-1753-YFP/$G\alpha_{i1}$·GDP·AlF$_4^-$-CFP interaction: $K_D = 0.76 \pm 0.08$ μM (best-fit ± std. error).
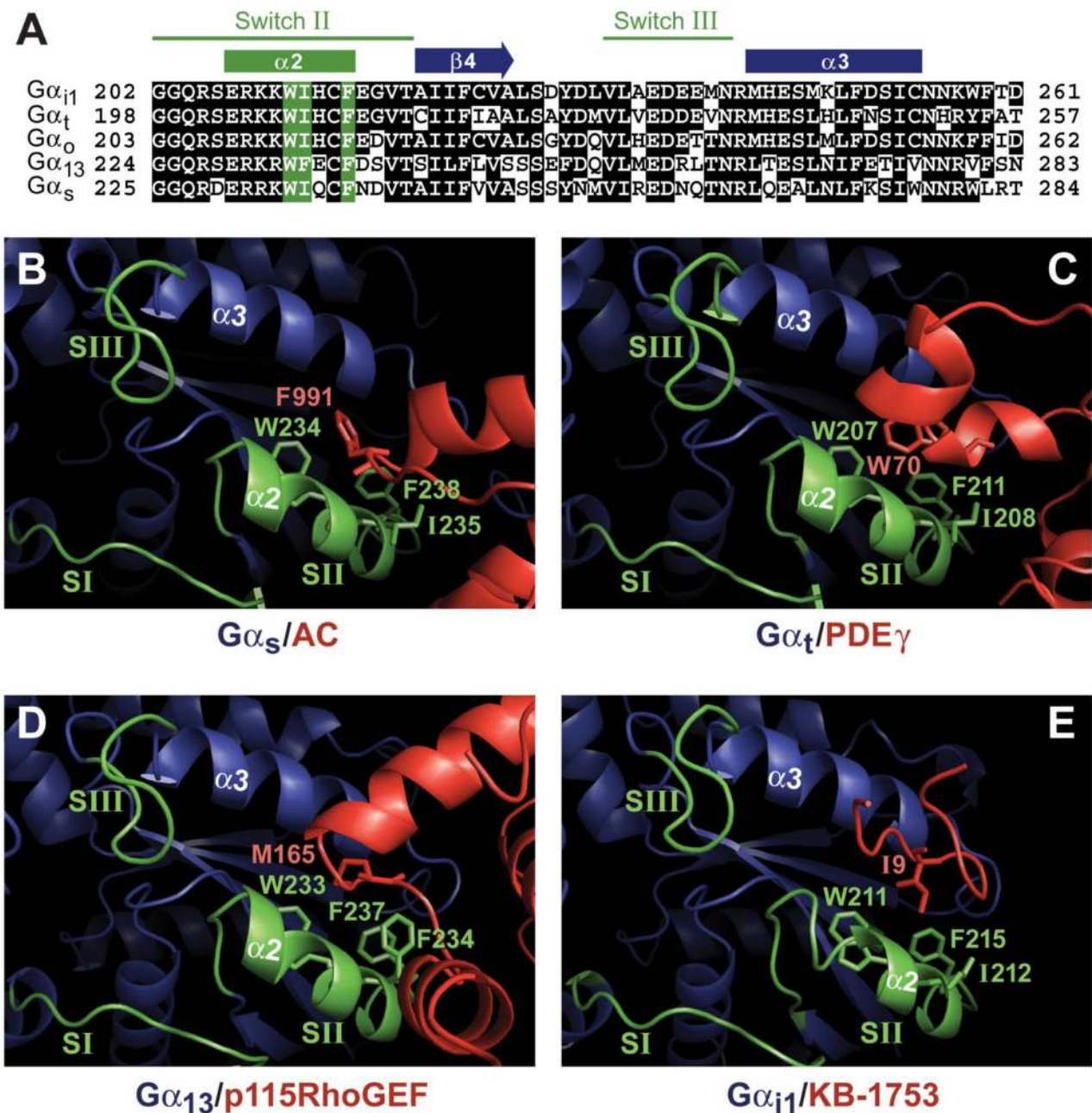
Figure 7. Conserved structural features of Gα engagement by effectors and by KB-1753
(**A**) Multiple sequence alignment derived from Clustal-X (59) of human Gα$_{i1}$ (GenBank AAM12619), bovine Gα$_t$ (SwissProt P04695), human Gα$_o$ (SwissProt P09471), human Gα$_{13}$ (GenBank NP_006563), and bovine Gα$_s$ (SwissProt P04896) sequences, highlighting locations of switch II and switch III, as well as conservation of three hydrophobic residues involved in effector engagement (green boxing). Burial of a key hydrophobic residue of an effector (red) within a conserved hydrophobic cleft between switch II (α2) and α3 helices of activated Gα (blue; switch regions in green) is apparent in the crystal structures of Gα$_s$·GTPγS bound to the second cytoplasmic domain of type II adenylyl cyclase (AC) (panel **B**; ref. 3), Gα$_t$·GDP·AlF$_4^-$ bound to the gamma subunit of cGMP phosphodiesterase (PDEγ) (panel **C**;

ref. 4), the N-terminal RGS domain of the RhoA guanine nucleotide exchange factor p115RhoGEF interacting with GDP·AlF$_4^-$-bound G$\alpha_{13/i\text{-}5}$, a chimeric Gα subunit based on Gα_{i1} but containing the three switch regions and the helical domain of Gα_{13} (panel **D**; ref. 5), and Gα_{i1}·GDP·AlF$_4^-$ bound to the KB-1753 peptide (panel **E**; this study).

Table 1

Data collection and refinement statistics

Data collection[a]	
Space group	P3$_2$21
No. of molecules per asymmetric unit	2
Unit cell dimensions	
a, b, c (Å)	103.13, 103.13, 206.99
α, β, γ (°)	90, 90, 120
Wavelength (Å)	1.1
Resolution (Å)	50-2.8 (2.9-2.8)
Linear R-factor[b]	0.093 (0.416)
Square R-factor[c]	0.065 (0.330)
Mean I/σ[d]	23.1 (2.7)
Completeness (%)	94.1 (61.0)
Redundancy	6.4 (4.5)
Refinement	
Resolution (Å)	50-2.8 (2.82-2.8)
No. reflections (working/test set)	25452/2824
R$_{work}$/R$_{free}$ (%)[e]	27.9/30.7
No. of non-hydrogen atoms	
Protein	5090
GDP/AlF/Mg	56/10/2
Water	30
R.m.s. deviations	
Bonds (Å)	0.01
Angles (°)	1.22
Average B-factor	51.4
Ramachandran plot (% in region)	
Allowed regions	98.9
Generously allowed	1.1
Disallowed	0.0

[a]Native data set collected at Brookhaven National Laboratory synchrotron X-ray source on Beamline x29. Numbers in parentheses pertain to the highest resolution shell.

[b]Linear R-factor = $\Sigma(|I - |)/\Sigma(I)$

[c]Square R-factor = $\Sigma(|I - |)^2/\Sigma(I)^2$

[d]<I/σI>, Mean signal-to-noise, where I is the integrated intensity of a measured reflection and σI is the estimated error in measurement.

[e]R$_{work}$ = $\Sigma(|F_p - F_{p(calc)}|)/\Sigma F_p$, where F$_p$ and F$_{p(calc)}$ are the observed and calculated structure factor amplitudes. R$_{free}$ is calculated similarly using test set reflections never used during refinement.